

Freeform LED lens for uniform illumination

Yi Ding, Xu Liu*, Zhen-rong Zheng, and Pei-fu Gu

State Key Laboratory of Modern Optical Instrumentation, Zhejiang University, Hang Zhou 310027, China

*Corresponding author: liuxu@zju.edu.cn

Abstract: Light flux from LED must be redistributed to meet the needs of lighting in most cases, a new method is proposed for its secondary optic design. Based on refractive equation and energy conservation, a set of first-order partial differential equations which represent the characters of LED source and desired illumination were presented. The freeform lens was constructed by solving these equations numerically. The numerical results showed that we can get a freeform lens for the illumination of uniformity near to 90%, with considerable high computation speed. This method can shorten the designing time of the freeform lens with high accepted tolerance.

©2007 Optical Society of America

OCIS codes: (080.4225) Nonspherical lens design; (080.4298) Nonimaging optics; (220.2945) Illumination design.

References and links

1. P. Zhou, W. Lu, Y. X. Lin, Z. R. Zheng, H. F. Li, and P. F. Gu, "Fly eye lens array used in liquid crystal projection display with high light efficiency," *Acta Optica Sinica* **24**, 587-591 (2004).
2. M. Shen, H. F. Li, W. Lu, and X. Liu, "Method of reflective fly eye lens design for LED illuminating projection system," *Acta Photonica Sinica* **35**, 93-95 (2006).
3. J. Bortz, N. Shatz, and D. Pitou, "Optimal design of a nonimaging projection lens for use with an LED source and a rectangular target," *Proc. SPIE* **4092**, 130-138 (2000).
4. B. A. Jacobson and R. D. Gengelbach, "Lens for uniform LED illumination: an example of automated optimization using Monte Carlo ray-tracing of an LED source," *Proc. SPIE* **4446**, 130-138 (2002).
5. B. Parkyn and D. Pelka, "Free-form illumination lens designed by a pseudo-rectangular lawnmower algorithm," *Proc. SPIE* **6338**, 633808 (2005).
6. H. Ries and J. Muschaweck, "Tailoring freeform lenses for illumination," *Proc. SPIE* **6338**, 633808 (2001).
7. H. Ries and J. Muschaweck, "Tailored freeform optical surfaces," *J. Opt. Soc. Am. A* **19**, 590-595 (2002).
8. Y. Ding and P. F. Gu, "The Freeform Reflector for Uniform Illumination," *Acta Optica Sinica* **27**, 540-544 (2007).
9. Y. Ding, X. Liu, H. F. Li, and P. F. Gu, "The design of the freeform reflector for uniform illumination," in *Proceedings of Asia Display 2007*, Volume 1. (Shanghai, China, 2007), pp. 735-738.
10. J. Schruben, "Formulation of a reflector design problem for a lighting fixture," *J. Opt. Soc. Am* **62**, 1498-1501 (1972).
11. W. H. Chen, *Introduction of Differential Geometry* (Beijing University, 1990), Chap. 4.
12. Y. C. Su and Q. G. Wu, *Numerical Solutions of Partial Differential Equations* (Weather, 1989), Chap. 1.
13. Lumileds LED technical data sheet, "Luxeon star technical data sheet" (Lumileds, 2006). <http://www.lumileds.com/pdfs/DS23.pdf>.
14. W. A. Parkyn, "Segmented illumination lenses for steplighting and wall-washing," *Proc. SPIE* **3779**, 363-370 (1999).
15. H. Chase, "Optical Design with Rotationally Symmetric NURBS," *Proc. SPIE* **4832**, 10-24 (2002).
16. T. L. R. Davenport, "3D NURBS representation of surface for illumination," *Proc. SPIE* **4832**, 293-301 (2002).
17. T. L. R. Davenport, "Generation of NC Tool Path for Subdivision Surface," in *Proceedings of CAD/Graphics 2001*, Q. Peng, ed. (International Academic, Kunming, China, 2001), pp. 1-7.
18. Precitech product features, "Freeform 700G" (Precitech, 2006). http://www.precitech.com/Precitech_ff700G_features.html.
19. Y. Z. Wang and L. J. Chen, "A real-time NURBS surface interpolator for 5-axis surface machining," *Chinese Journal of Aeronautics* **18**, 263-272 (2005).

1. Introduction

The application of light emitting diodes (LED) in projection display system has become more and more important with the continuous increase of the luminous flux of single LED. But the traditional illumination system may not work well with LED in most cases because of its light

distribution. The direct output of an LED is normally a circle spot while the desired illumination in projector is always a rectangular form, which would cause large energy loss. Usually some optical elements, for example integrators, are applied to change the circle illumination into rectangle form, such as fly eyes or light tubes in LCD projectors [1, 2]. But multiple reflection or refractions in these elements also would cause loss. Freeform optical components are considered as the best technique to get the desired illumination. There are two methods to design the freeform lens: one is the trial and error method, which always requires a lot of time [3, 4]. The other is to construct the lens using the non-imaging tailoring method [5, 6]. These methods have lots of limitations, not only on the limit of forming the desired illumination, but also on the time consuming in the calculation. Especially, for the application of projection display, it needs a high uniform rectangular illumination. And it is hard to use the above methods to meet the needs.

Usually people use reflective design to perform similar task, but considering the luminous angel of LED can extend to 180° , and the encapsulation and circuit board attached to the LED could be comparatively large, it would not be easy to reflect the light without block, so lens is always a preference for LED illumination. In this paper, a new freeform optical lens design method is proposed. Based on the Snell's law and the energy conservation [6-9], we can deduce from the characteristics of the source and the desired illumination, to get a set of first-order partial differential equations. By solving these equations numerically, we can get the refractive freeform lens. The method can be used to design a freeform lens in a fast way (just less than 20 seconds on a common PC). Using an LED as the source, a uniform rectangular form illumination can be gotten through single refractive freeform lens, and with illumination uniformity near to 90%. The rectangular illumination also has a relatively clear cut-off line with little blur at the edge. It means that one can get the desired illumination form with high precision and with high efficiency. Moreover, this method can not only create uniform rectangular illumination, but also many other form of illumination, such as octagon form illumination for example.

2. Partial differential equation sets

Assuming that the center of LED source \mathbf{S} is located at the origin of an orthogonal coordinate system, so points on the target plane \mathbf{T} for the illumination can be expressed as $t(x, y, z)$. The freeform lens \mathbf{P} is located in a spherical coordinate system, which shares the same origin with the orthogonal system mentioned above [10]. Thus, the coordinates on \mathbf{P} are $(\theta, \varphi, \rho(\theta, \varphi))$, and the normal vector at point p of the lens is \mathbf{N} . Assume \mathbf{I} is the vector of the incident light at point p , while \mathbf{O} is the vector of refractive light by the freeform lens from point p to point t . Figure 1 shows the relationships between these vectors.

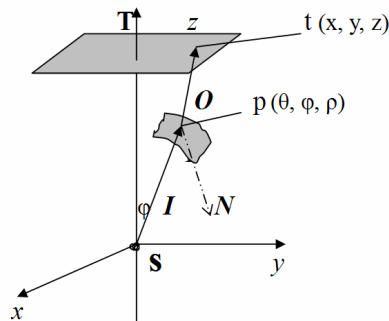


Fig. 1. Vectors in refraction.

2.1 Refractive vectors

If we take \mathbf{N} , \mathbf{I} and \mathbf{O} as the unit vectors of normal, incident and refractive vectors respectively, and they can be expressed as:

$$\mathbf{N} = (N_x \mathbf{i}, N_y \mathbf{j}, N_z \mathbf{k}). \quad (1)$$

$$\mathbf{I} = (I_x \mathbf{i}, I_y \mathbf{j}, I_z \mathbf{k}). \quad (2)$$

$$\mathbf{O} = (\mathbf{t} - \mathbf{p}) / |\mathbf{t} - \mathbf{p}|. \quad (3)$$

These three vectors are connected to each other via the Snell's law. Here \mathbf{O} has connections with the position of point \mathbf{p} and \mathbf{t} . After using Snell's law at the point \mathbf{p} , we have the equations as shown in Eqs. (4) and (5):

$$x = N_x \left[n_o (z - p_z) - n_l I_z |\mathbf{t} - \mathbf{p}| \right] / (n_o N_z) + p_x + n_l / n_o I_x |\mathbf{t} - \mathbf{p}|. \quad (4)$$

$$y = N_y \left[n_o (z - p_z) - n_l I_z |\mathbf{t} - \mathbf{p}| \right] / (n_o N_z) + p_y + n_l / n_o I_y |\mathbf{t} - \mathbf{p}|. \quad (5)$$

Here, n_l and n_o indicate the refractive index of the incidence and emergence medium. \mathbf{I} can be expressed by ρ , θ and φ . Equations (4) and (5) are the partial differential equations used for the freeform lens calculation. And the subscript of N include the first-order partial derivative of $\rho(\theta, \varphi)$ on the directions of θ and φ , which stands for the slope at point \mathbf{p} of the freeform lens [11]. It could be calculated from:

$$\mathbf{N} = (\rho_\theta \otimes \rho_\varphi) / |\rho_\theta \otimes \rho_\varphi|. \quad (6)$$

And the subscript of p is the vector component of \mathbf{p} on x, y and z directions. In orthogonal coordinates they can be expressed as:

$$\mathbf{p} = (p_x, p_y, p_z) = (\rho(\theta, \varphi) \sin \varphi \cos \theta, \rho(\theta, \varphi) \sin \varphi \sin \theta, \rho(\theta, \varphi) \cos \varphi). \quad (7)$$

2.2 Energy conservation

According to light transmission energy conservation condition, the output of source is equal to the flux incident in the target plane. Assuming the half viewing angle of the source is φ_{MAX} :

$$\int_0^{2\pi} d\theta \int_0^{\varphi_{MAX}} I(\mathbf{I}(\varphi)) \sin \varphi d\varphi = \int E(\mathbf{t}) dA. \quad (8)$$

where $E(\mathbf{t})$ is the luminance at point \mathbf{t} , A is the area illuminated. $I(\mathbf{I}(\varphi))$ is LED emitting intensity in the direction of $\mathbf{I}(\varphi)$. Equation (8) indicates the relationship between θ , φ and x , y , z , and its exact form depends on the topological mapping from the source to the target plane.

When target plane \mathbf{T} is fixed, θ and φ can be gotten through Eq. (8). After replacing the corresponding items in Eqs. (4) and (5) by θ and φ , the first-order partial differential equation sets of $\rho(\theta, \varphi)$ on the directions of θ and φ can be deduced. It is difficult to obtain the analytic solution from these partial differential equations, so numerical methods are employed [12].

3. Freeform lens design

In this section, a LUXEON Star LED (LXHL-MM1D) will be taken as the light source to design a freeform lens. This LED has an analogous Lambertian radiation distribution, with the die size of $1 \times 1 \text{ mm}^2$ [13]. In order to simplify the calculation, we assume that the top surface of LED die is in the x - y plane and its center is located at the origin. The target plane \mathbf{T} is a rectangle with the ratio of 4:3. It's perpendicular to the z -axis, and its center is $(0, 0, 30)$.

Assuming that a lens with one spherical surface and one freeform surface, and of the refractive index 1.5, is located in front of the LED die, and the spherical surface is facing the LED, whose radius is 50 mm, center is $(0, 0, -45)$ and vertex $(0, 0, 5)$, the vertex of the freeform surface is $(0, 0, 10)$, just as Fig. 2(a) shows.

MM1D could be equivalent to a surface-emitting rectangle with specific intensity distribution versus angle. The incident vector on freeform surface is:

$$\mathbf{I} = (\sin \varphi_l \cos \theta_l \mathbf{i}, \sin \varphi_l \sin \theta_l \mathbf{j}, \cos \varphi_l \mathbf{k}). \quad (9)$$

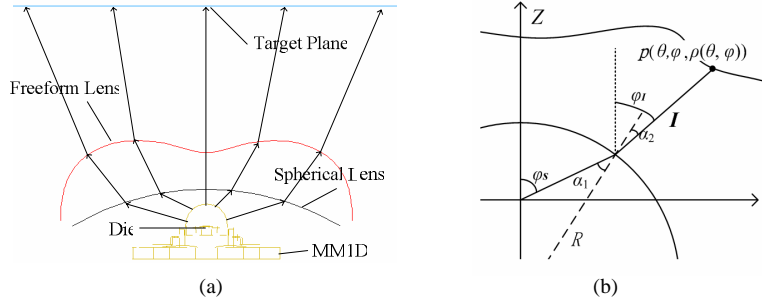


Fig. 2. The LED refractive illumination system.

If we take LED as a point source, and assume that the polar angle of light from point source is φ_s , and angles of incidence and refractive on the spherical surface are α_1 and α_2 , just as Fig. 2(b) shows. It's easy to get that:

$$\varphi_I = \varphi_s - \alpha_1 + \alpha_2. \quad (10)$$

Because this spherical surface didn't change the θ value of light from a point source, with equivalent θ , the relationship among freeform surface and φ_s , α_1 , α_2 can be shown as:

$$\frac{\rho}{\sin(\alpha_1 - \alpha_2)} = \frac{\sin(\varphi_s - \alpha_1) \times R}{\sin \varphi_s \sin(\alpha_1 - \alpha_2 - \varphi_s + \varphi)}. \quad (11)$$

where R is the radius of the sphere, and α_1 , α_2 can be expressed by φ_s through analytic geometry and the refraction law. If a point p on freeform surface is known, for example, the vertex point, then φ_s can be got according to Eq. (11). Thereby get \mathbf{I} through Eqs. (9) and (10).

In this paper the light distribution of MMID is an assembly of measuring data, which are luminous intensity values in different φ directions, and can be considered as constant in the range of $\varphi_n \pm d\varphi/2$. Assume the intensity in direction of φ_n as $I(\mathbf{I}(\varphi_n))$, and the number of measuring points is N , then the luminous flux of LED between φ_0 and φ_N can be expressed as:

$$\Phi_{LED} = 2\pi \times \left(\int_{\varphi_0}^{\varphi_0 + \frac{d\varphi}{2}} I(\mathbf{I}(\varphi_0)) \sin \varphi d\varphi + \sum_{n=1}^{N-1} \int_{\varphi_n - \frac{d\varphi}{2}}^{\varphi_n + \frac{d\varphi}{2}} I(\mathbf{I}(\varphi_n)) \sin \varphi d\varphi + \int_{\varphi_N - \frac{d\varphi}{2}}^{\varphi_N} I(\mathbf{I}(\varphi_N)) \sin \varphi d\varphi \right). \quad (12)$$

where $d\varphi = (\varphi_N - \varphi_0)/N$, $\varphi_n = \varphi_0 + n \cdot d\varphi$. In uniform illumination, $E(t)$ in Eq. (8) is a constant. The topological mapping applied is showed in Fig. 3, which means lights of equal φ would be refracted to the same edge of the rectangle [14]. After substituting Eq. (12) into Eq. (8):

$$\Phi_{LED} = E \times 4 \times X \times Y \quad (X/Y = 4/3). \quad (13)$$

where X and Y are the coordinates of the corner of the rectangle, and both of them are >0 . After φ_s is confirmed, Φ_{LED} would be known. Then θ in the first quadrant can be expressed as:

$$\begin{cases} \theta = \frac{y'}{Y} \times \frac{\pi}{4} & 0 \leq \theta \leq \frac{\pi}{4} \\ \theta = \frac{X - x'}{X} \times \frac{\pi}{4} + \frac{\pi}{4} & \frac{\pi}{4} \leq \theta \leq \frac{\pi}{2} \end{cases}. \quad (14)$$

where x' and y' are coordinates on the target plane, and the values of θ in the other quadrants can be easily calculated by the same way.

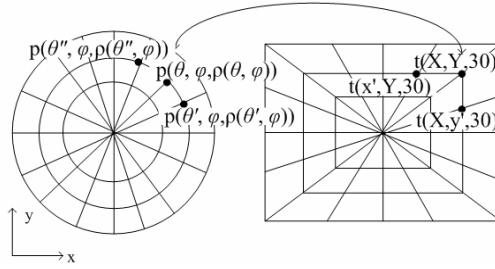


Fig. 3. The topological mapping from source to target plane.

Because it's difficult to calculate φ_s through Eq. (13) from $X, Y, d\theta$ and $d\varphi$ are applied to discretize the source, Then the polar and azimuth angle of light from source become:

$$\varphi_s = n \times d\varphi; \quad \theta_s = i \times d\theta. \quad n, i = 0, 1, 2, \dots \quad (15)$$

Then substituting Eqs. (10) and (11) into Eq. (9), I became function of $\rho(\theta, \varphi)$, so that the incident position on the target plane can be calculated through Eqs. (12), (13) and (14). Thereby the unknowns of Eqs. (4) and (5) become $\rho(\theta, \varphi)$ and its first-order derivatives in the direction of θ, φ . Using the difference scheme of $\rho(\theta, \varphi)$ to replace its first derivatives, while discretizing the equations with φ_s and θ_s and the grids depicted in Fig. 3, the partial differential equation sets turn into a set of nonlinear equations whose unknown is $\rho(\theta_s, \varphi_s)$.

It only takes about 20 seconds to solve equations using a computer with a 2.40 GHz Celeron CPU, and the numerical results stand for the contour of the freeform lens.

The freeform surface can be modeled using non-uniform rational B-splines (NURBS), which offers a common mathematical form representing and designing freeform surfaces [15, 16]. Theoretically the freeform surface constructed from these data should be smooth. But in practice, if the freeform surface was modeled as a whole, the simulated result was not good.

This problem could be avoided by modeling the surface with discrete sub-surfaces, as Fig. 4 shows. Here the freeform lens consists of 450 pieces. Each piece is lofted from 3 lines which are constructed from points. Points on the central line are calculated in the direction of φ , while points on the two fringe lines are calculated in the direction of θ . All 3 lines cross at the vertex point of the freeform lens, which means 450 sub-surfaces share the same vertex. And the more sub-surfaces, the better simulated results. But too many sub-surfaces would cost much time to model them, so 450 are just fine. The projective length of freeform lens on the x-axis is about 40 mm, on the y axis it is about 36 mm, and its height is about 10 mm.

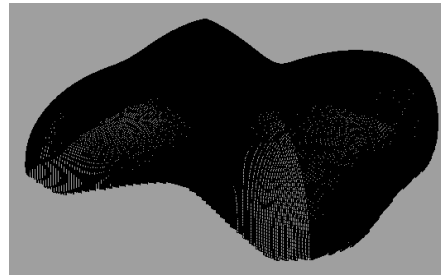


Fig. 4. The freeform lens.

Once we get the free form lens, we can use ASAP to simulate and verify the illumination results of the freeform lens illumination performance. Figure 5 shows the simulated results of 1 million light rays tracing.

It is shown in the Fig. 5(a) that the rectangular illumination on the target plane, which is a 4:3 rectangle whose diagonal length is about 100 mm. And Fig. 5(b) shows the energy

distribution cross the center and the quarter of the rectangle in x directions. The vertical axis in graphs stands for the normalized illumination, while the horizontal stands for the x axis.

From Fig. 5(b), we can see that the uniformity across the center is quite well, near 90%. The energy inside the desired rectangle is about 95.56% of the output of the source, in case of no refraction loss. But there's still some insufficiency: the illumination on the diagonal of the rectangle is a little lower compared with their surroundings according to Fig. 5, which was caused by the absorptions of the gaps between those sub-surfaces of the freeform lens. And the uniformity in this region dropped to about 85%.

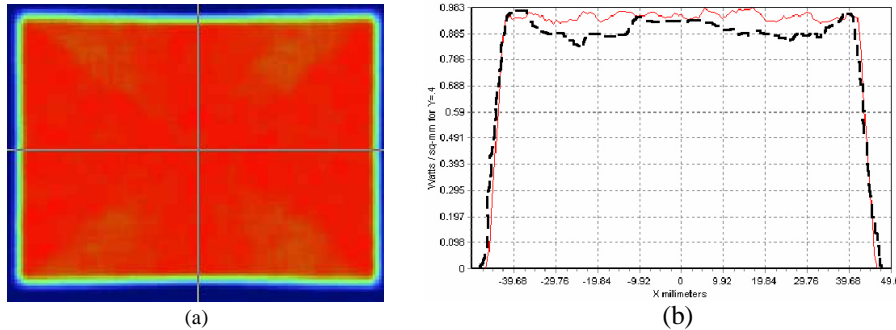


Fig. 5. The simulated results using MM1D as the source. — across the center; — across the quarter.

Not only limit to rectangle, this method can also be used to design freeform lens illuminating different forms, such as octagon. Figure 6 shows that the same LED forms an octagon. We can also get a uniform illumination with very good clear boundary.

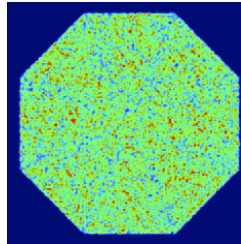


Fig. 6. The simulated results of an octagon illumination.

4. Tolerance analysis

The tolerance of a freeform lens is an important issue in the freeform optical component design. In this illumination case the tolerance analysis will be focused on the source radiation, source translation, and the surface tooling errors.

The source radiation used in Fig. 5 is not a Lambertian. If the LED radiation becomes a $1 \times 1 \text{ mm}^2$ Lambertian rectangle, one can get the target illumination as shown in the Fig. 7. Comparing with the result in Fig. 5, the uniformity has been influenced when the radiation turn to Lambertian. Figure 7(b) shows the illumination uniformity across the center is about 80%, and uniformity on the quarter line near the diagonal region is 75%. In fact the illumination difference between MM1D and a Lambertian source is much larger than the fluctuation among the real sources, so the uniformity would be higher than 80% in actual application.

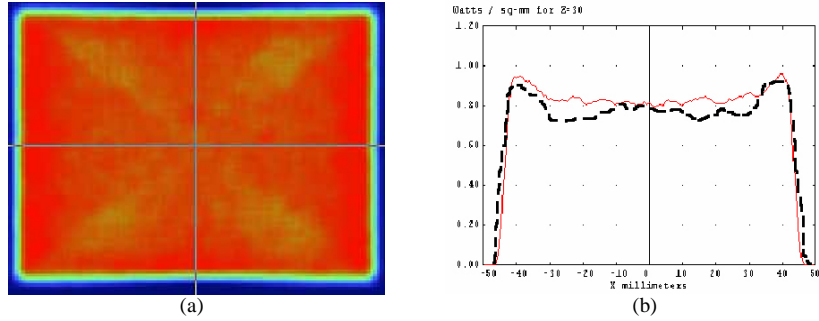


Fig. 7. The simulated results using a $1 \times 1 \text{ mm}^2$ Lambertian rectangle as the source. — across the center; — across the quarter.

The influence of LED's position to the illumination is shown in Fig. 8. When the LED source was translated along $+x$, $+y$, $+z$ and $-z$ directions for 0.1 mm respectively, the illumination form keeps as a rectangular form. It seems that the illumination is not sensitive to the y axis and x axis displacements of the source, and improved a little when the source was translated along $-z$ axis. Anyway the illumination isn't sensitive to the positioning errors of LED.

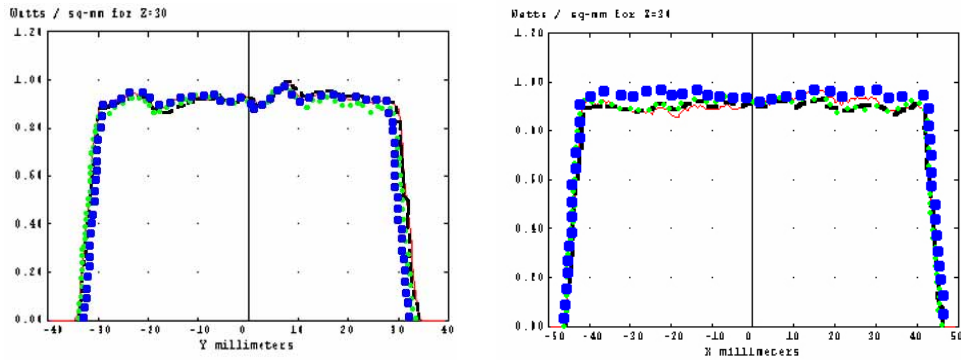


Fig. 8. The illumination distribution when the source was translated for 0.1mm. — along $+x$ axis; — along $+y$ axis; ● along $+z$ axis; ■ along $-z$ axis.

It seems that the illumination is more sensitive to the source rotation. Figures 9(a) and 9(b) show the illumination distribution across the center of the target plane along x and y axis, when the LED source was rotated round the x axis, y axis and vector $(1, 1, 0)$ for 3° .

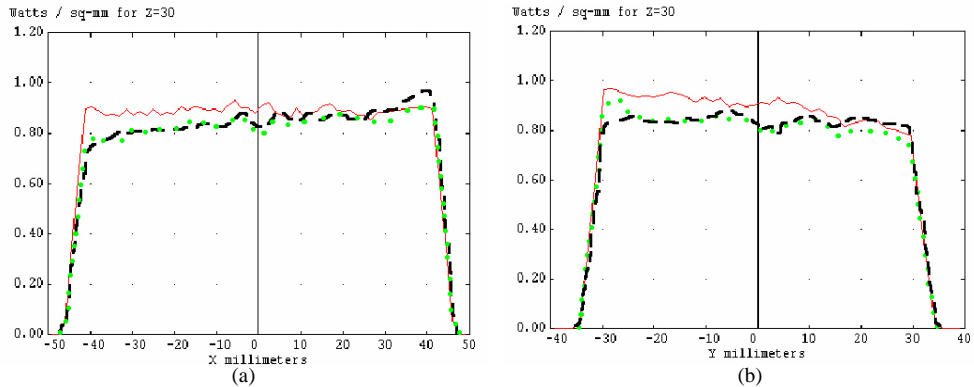


Fig. 9. The simulated results when the source was tilted 3° . — rotation round x axis; — rotation round y axis; ● rotation round vector $(1,1,0)$.

We can see that when the source rotated round x axis for 3° , the illumination along y axis deteriorated. The uniformity on the right dropped to about 75%. And this also happened to the illumination along x axis when the source was rotated round y axis. The deterioration caused by rotation round vector (1, 1, 0) is similar to that by rotation round y axis. 3° is fairly large error when one assembles a lens, so that this lens is not quite sensitive to the rotation errors.

The freeform surface in this paper was constructed from a series of points. In order to simulate the surface tooling errors, we manually change the values of these points: add an $F[n]$ to $\rho(\theta, \varphi)$ of each point. $F[n]$ can be expressed as $F \times \sin(2\pi/T \times n)$, where F is used to simulate the degree of the surface error, and T to simulate the frequency of the fluctuation. Figure 10(a) shows the illumination distributions along x axis when F was set to $0.1 \mu\text{m}$. When T was set to 10, 50 and 100, the results changed respectively.

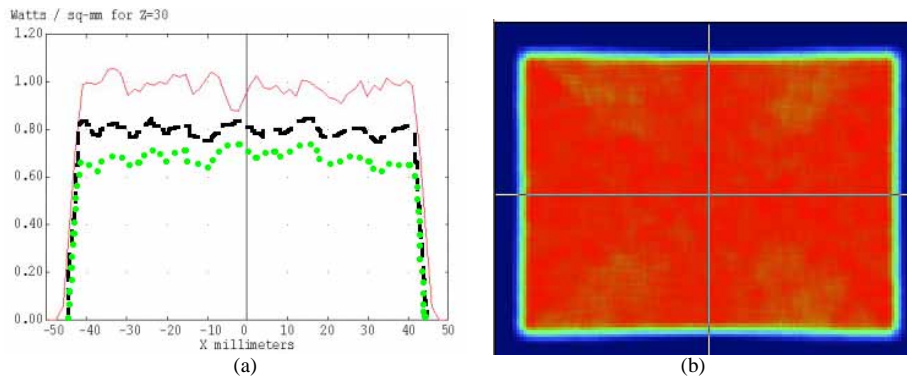


Fig. 10. The simulated results when F is $0.1 \mu\text{m}$. — $T=100$; — $T=50$; • $T=10$.

It seemed like that the gentler the fluctuation, the better the result. The illumination on the target plane when $T=100$ is showed in Fig. 10(b), with a uniformity around 90%. Figure 11 shows the simulation results when F was extended to $2 \mu\text{m}$, while $T=100$.

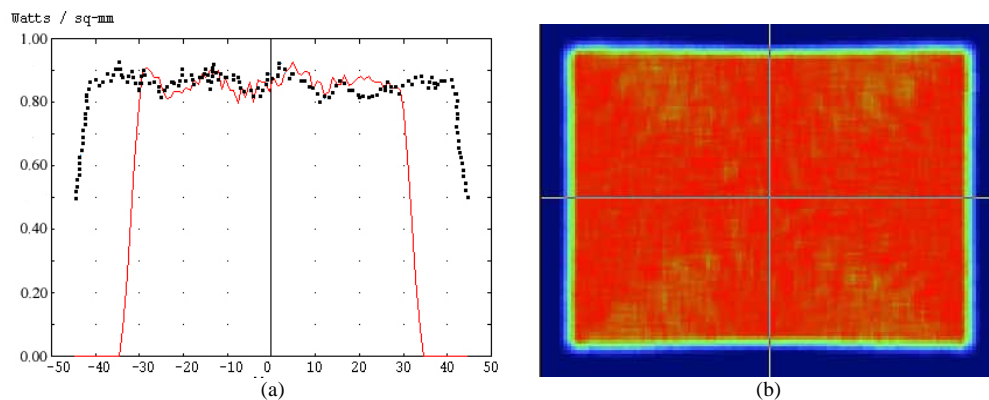


Fig. 11. The simulated results when F is $2 \mu\text{m}$. — illumination along x axis; • illumination along y axis.

As from the pictures above, the uniformity dropped to 85% when the degree of surface error was extended to $2 \mu\text{m}$. And the region around diagonal line deteriorates most of all.

5. Conclusion

The first-order partial differential equation sets proposed in this paper can be applied to construct a freeform lens for uniform illumination of various forms, given the characters of the source and the desired illumination. The numerical results of equations stand for the figure of the freeform surface. Without professional optical designing software, it only takes about 20 seconds to obtain the solution by C programming language and the simulated uniformity is quite good. The tolerance analysis simulations show that the illumination didn't deteriorate too much when the intensity distribution and the position of the source changed. And if the fluctuation of errors on surface has a low frequency, the surface tolerance can be up to 2 μm . And the ultra precision multi-axes diamond machining systems make the manufacture possible.

The clear cut-off line of the illumination can not only help to reduce the energy loss in the special form illumination, but also can be quite useful in some particular situations where a clear cut-off line desired, such as the dipped headlight. Moreover this method can create various uniform figures, broadening the scope of freeform lens's usage.